Science and Engineering Research Council
Rutherford Appleton Laboratory
CHILTON, DIDCOT, OXON, OX11 0QX

RAL 86-068

Initial Results from the High Resolution Powder Diffractometer HRPD at ISIS

W I F David, W T A Harrison and M W Johnson

July 1986

INITIAL RESULTS FROM THE HIGH RESOLUTION POWDER DIFFRACTOMETER, HRPD AT ISIS

W I F David, W T A Harrison and M W Johnson
Neutron Division
Rutherford Appleton Laboratory
Chilton Didcot
Oxon OX11 0QX

ABSTRACT

This paper reviews the initial commissioning of the high resolution time-of-flight neutron powder diffractometer, HRPD, on the Spallation Neutron Source, ISIS, at the Rutherford Appleton Laboratory. Preliminary results have confirmed both intensity and resolution predictions indicating that ($\Delta d/d$) lies between 0.04% and 0.08% for all d-spacings between 0.2 and 5Å. The scientific potential of this increased resolution over existing time-of-flight diffractometers has been demonstrated in the successful ab initio structure determination of an unknown inorganic material, $FeAsO_4$, and the detailed study of subtle symmetry changes in NiO. The true instrumental resolution, however, has been observed in only a small number of experiments: sample broadening is often seen to play a dominant role in the determination of the peak shape, particularly at longer d-spacings. This leads to additional useful information about macroscopic properties, such as anisotropic crystallite size, strain distribution and sample homogeneity, but also results in a significant increase in complexity of peak-shape description and data-analysis strategy.

INTRODUCTION

High resolution time-of-flight (TOF) powder diffraction on pulsed neutron sources has developed rapidly over the past five years to become a complementary technique of comparable power to conventional neutron and X-ray powder diffraction. This is principally as a result of the routine operation of the Special Environment Powder Diffractometer (SEPD) and General Purpose Powder Diffractometer (GPPD) at the IPNS, Argonne National Laboratory, USA and the successful application of the Rietveld method to data collected on these machines [1]. The high resolution powder diffractometer, HRPD, at ISIS has an improvement in resolution of 5-7 over GPPD and SEPD and represents the first of a new generation of neutron diffractometers with a ($\Delta d/d$) resolution less than 0.001.

In order to achieve ($\Delta d/d$) resolutions of around 0.0005 the primary flight-path of a TOF diffractometer must be of the order of 100 m. On a pulsed source operating at 50 Hz this introduces problems of multiple frame overlap that are eliminated by using beam choppers. HRPD has been designed with two disk choppers situated at 6.135 m and 9.2 m from the moderator. The first chopper, which rotates at ISIS frequency (50 Hz), has 3 slots that allow through 1, 2 and 5 frames (19.5 ms, 39.5 ms and 99.5 ms at 98 m respectively). The second chopper, running at (50/N) Hz, allows through one in N frames where N = 1,2,5. These three configurations correspond to wavelength windows of 0.79 Å, 1.59 Å and 4.02 Å respectively, which may be moved to higher or lower wavelengths by phasing the choppers relative to the initial neutron pulse.

The primary flight-path of HRPD is enclosed within a curved nickel-coated glass guide of cross-section 8 cm x 2.5 cm to attenuate the γ rays and fast neutrons associated with the initial burst. The curved section of the guide, which extends from 6 m to 60 m from the moderator, has a radius of curvature of 18 km. These parameters represent the optimised configuration for a 50 Hz source in which no line-of-sight neutrons reach the sample yet the radius of curvature is sufficiently shallow to allow the transmission of sub-angstrom neutrons. The 60 m - 90 m straight section of the guide is necessary to smooth out beam inhomogeneities in the guide. No neutrons are transmitted below $\lambda < 0.48$ Å; when $\lambda > 5$ Å the flux varies as $\sim \lambda^{-5}$.

A schematic drawing of HRPD is given in Figure 1. Two sample positions are available, at 1 m and 2 m from the backscattering bank of detectors, with vertical access to both positions for sample environment instrumentation. In addition a low-angle bank will be installed in July 1986 and a 90° detector bank is under consideration. The backscattering detector at present consists of 2 of a final 8 octants that will form a series of 20 concentric detector rings that match the Debye-Scherrer cones thereby eliminating asymmetrical geometrical contributions to the profile line-shape.

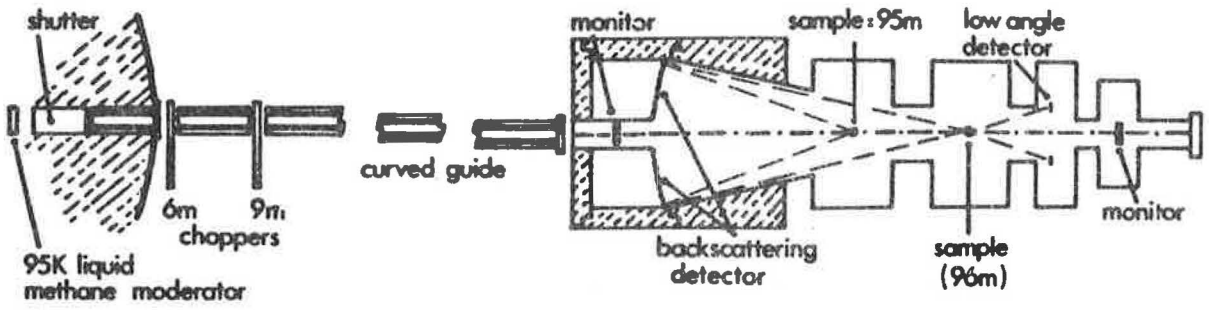

Figure 1: Schematic plan of HRPD showing beam choppers, curved guide section and backscattering detectors as described in the text.

HRPD RESOLUTION AND PEAK SHAPE

Resolution

The resolution of HRPD arises from a combination of different physical variables, and a detailed discussion of the matching of the different instrumental parameters is given elsewhere [2]. A simplified account of the resolution contributions to ($\Delta d/d$) assumes that all variables are independent such that:

$$(\Delta d/d)^2 = (\Delta t/t)^2 + (\Delta \ell/\ell)^2 + (\Delta\theta \cot\theta)^2 + (d/p)^2 + \varepsilon^2$$

$\Delta t/t$ arises from the time distribution of the neutron pulse resulting from the moderator, and optimisation studies [3] have led to the choice of a 10 cm x 10 cm 95 K liquid methane moderator poisoned by gadolinium to a depth of 2 cm, resulting in a 'tight' neutron pulse time structure over a wide range of wavelengths. $\Delta\ell$ is the uncertainty in the flight path ℓ and results from finite sample and detector thicknesses. For ℓ = 98 m, this term is of the order of 0.0001. The geometrical resolution $\Delta\theta \cot\theta$ resulting from finite sample and detector sizes is less than 0.001 only for $\theta > 80°$ necessitating a very high-angle detector bank. At the 1 m position the angular resolution is $\approx$ 0.0006 whilst for the 2 m position, $\Delta\theta \cot\theta \sim 0.00015$. Thus, neglecting strain broadening, ε, and particle size effects, d/p, where d is the d-spacing and p the crystallite diameter, the predicted 1 m and 2 m resolutions are of the order of 0.001 and 0.0005 respectively. The predicted and measured upper limit resolution curves for a nickel oxide sample at the 2 m position are illustrated in Figure 2. The experimenter has a choice between higher resolution (2 m position) or a four-fold gain in intensity with lower resolution at the 1 m position.

Peak Shape

The peak shape in neutron time-of-flight powder diffraction is more complex than that for the constant wavelength case, and must take account of the contributions of moderator, diffractometer geometry and the effect of the sample. The time structure of neutrons of a particular wavelength leaving the moderator is well modelled by the Ikeda-Carpenter function [4], which must be convoluted with Gaussian instrumental and Lorentzian sample contributions. This may be approximated by a convolution of the Ikeda-Carpenter function with a pseudo-Voigt function, to be fully described later [5]. Although mathematically complex, the resulting function is a correct physical model for the peak shape, and has been highly successful in fitting individual peaks for a wide range of samples, with extraction of physically reasonable values for macroscopic sample parameters, as well as the expected moderator and geometrical terms.

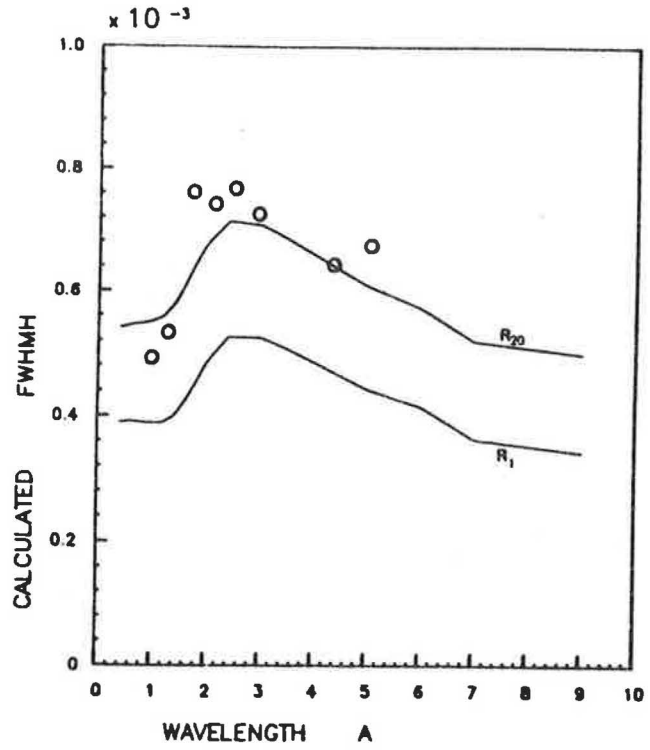

Figure 2: Predicted (lines) and measured (circles) full width at half maximum height resolution curves for HRPD at the 2m scattering position as a function of wavelength. Resolution is highest for the inner detector rings which are closest to backscattering geometry. The nickel oxide resolution has been measured from summed spectra.

STRUCTURAL PHASE TRANSITIONS

The almost constant ($\Delta d/d$) resolution of TOF diffractometers makes them ideal instruments for the study of structural phase transitions. In the absence of sample broadening, subtle peak splittings associated with lowering of symmetry may be observed with roughly equal precision in multiple order (nh nk nℓ) of the same fundamental (h k ℓ) reflection. Thus lattice distortions may, in contrast to conventional instruments, be observed with very high precision in low-index reflections, where the overall density of peaks is very low.

Nickel oxide is an ideal candidate to test resolution. The simple cubic rock salt structure is distorted to monoclinic or possibly triclinic symmetry by the onset of antiferromagnetic ordering at 525K. In practice, the structure appears to be rhombohedral, producing a splitting of peaks across the whole diffraction pattern requiring a resolution of 10^{-3} at room temperature. To date, these splittings have not been resolved by any other neutron powder diffractometer. Figure 3 shows the $(111,1\bar{1}\bar{1})$ and $(222,2\bar{2}\bar{2})$ doublets both observed at a resolution of less than 6×10^{-4}. From the fitted peak positions, as listed below, the rhombohedral α angle has been refined to high accuracy and precision.

In contrast, the (h00) peaks (h = 2n) showed no perceptible splitting, indicating that the monoclinic distortion must be less than 10^{-4} in magnitude. These results have also been confirmed by recent synchrotron measurements on the same sample[6].

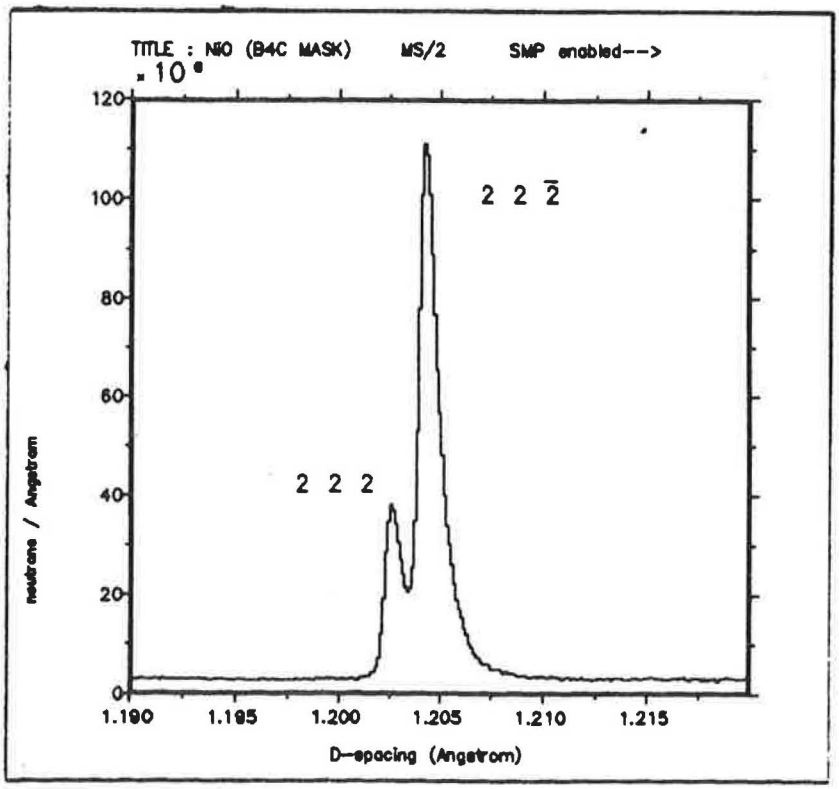

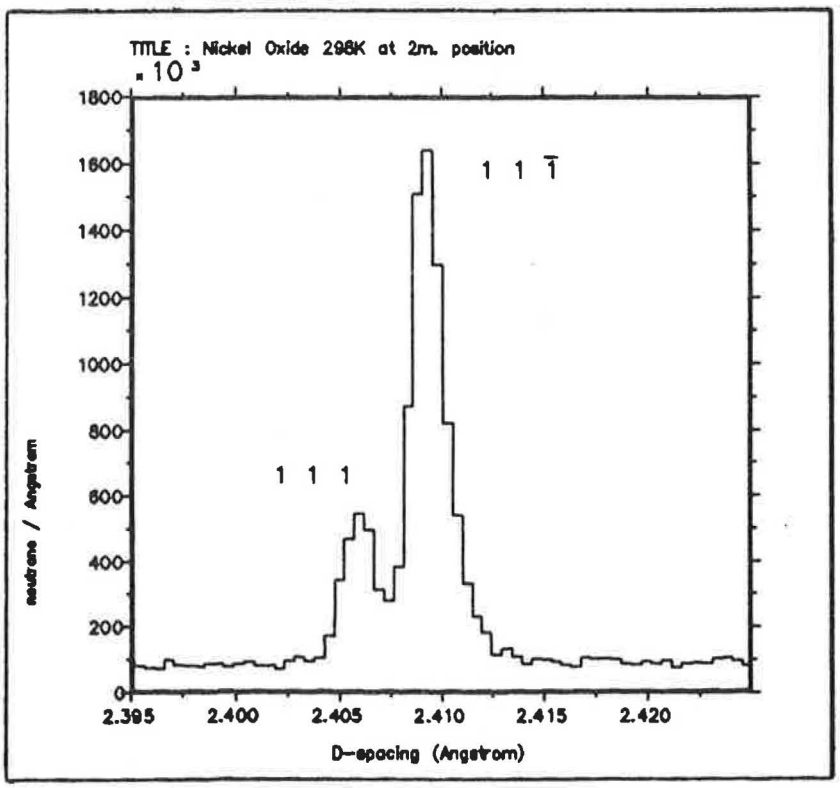

Figure 3: The $(111,11\bar{1})$ and $(222,22\bar{2})$ doublet reflections of nickel oxide plotted as a function of d-spacing

Nickel Oxide room-temperature cell constant refinement

h	k	l	Obs TOF	Calc TOF	Diff	Error
2	-2	0	73110.23	73110.64	-0.42	1.49
2	2	0	73033.31	73033.10	0.20	1.50
2	2	-2	59684.76	59684.67	0.08	0.60
2	2	2	59600.37	59600.34	0.03	0.60
4	0	0	51669.73	51670.03	-0.30	1.88
4	-2	0	46234.28	46234.34	-0.05	0.58
4	2	0	46195.08	46195.11	-0.02	0.60
4	-4	0	36554.55	36554.11	0.43	1.00
4	4	0	36515.03	36515.33	-0.29	1.00

Refined lattice constants:

$a = 4.1749(3)$ Å $\qquad \alpha = 90.0608(15)°$

SAMPLE BROADENING

Diffraction Studies of $Rb_2(FeTi)PO_4)_3$

$Rb_2(FeTi)(PO_4)_3$, a synthetic primitive-cubic langbeinite ($a \simeq 10$ Å : space group $P2_13$), was examined as part of the calibration of the long wavelength diffraction spectrum on HRPD and indicated a useful neutron flux d-spacing up to $\lambda \approx 12$Å. In addition to providing the suitable well spaceed long d-spacing reflections for such a calibration, $Rb_2(FeTi)(PO_4)_3$ was chosen because of its potential scientific interest as an order-disorder structure. Langbeinite may be regarded as a lower-symmetry variant of garnet (space group Ia3d : e.g. $Ca_3Al_2(SiO_4)_3$) in which two of the three 24c (Ca) sites are occupied in an ordered manner because of the buckling of the corner-linked octahedral/tetrahedral $M_2(XO_4)_3$ framework to accommodate the very large monovalent cation (Rb). This distortion results in two crystallographically-distinct but chemically-similar octahedral sites over which the Fe and Ti ions may either order or disorder. Although determination of the order/disorder character of $Rb_2(FeTi)(PO_4)_3$ is greatly facilitated by the large difference in Fe (9.54 fm) and Ti (-3.37 fm) scattering lengths, the diffraction data indicated a complex sample-broadened peak shape that was common to all reflections (Figure 4). Rather that the anticipated sharp leading edge and slow exponential decay, each peak showed a pronounced slow rise indicative of a strain distribution. Initially this was attributed to the presence of a second langbeinite phase at the 5% level because of the successful modelling of a biphasic distribution to individual peaks. This yielded a fractional lattice constant change of $(\Delta a/a) = 0.00155$. Detailed analysis of this peak description, however, indicated that a two-phase model was inadequate and that a continuous distribution of local ordering/concentration variation of Fe and Ti was more likely. However, as the nature of the sample broadening is uncertain, analytical peak-shape refinement was deemed unsuitable and an alternative procedure involving maximum-entropy deconvolution was employed [7]. Initial results confirm a continuous distribution resulting from strain broadening.

As a result of the problems encountered in peak-shape description the average structure was refined from 64 extracted integrated intensities by grouped-

intensities least-squares analysis (GRILS) based on the Mark III version of the Cambridge Crystallographic Subroutine Library [8]. The resulting structural parameters are listed below: the atomic coordinates are typical of previous langbeinite studies [9,10]; no evidence of Fe/Ti ordering was found as the Fe/Ti occupancies refined to a random model.

$Rb_2(FeTi)(PO_4)_3$ langbeinite: final atomic parameters

Atom	x/a	y/b	z/c	Fe occ.
Rb(1)	0.060(1)	0.060(1)	0.060(1)	
Rb(2)	0.289(1)	0.289(1)	0.289(1)	
Fe/Ti(1)	0.596(4)	0.596(4)	0.596(4)	0.503(13)
Fe/Ti(2)	0.852(3)	0.852(3)	0.852(3)	0.497(13)
P	0.626(2)	0.457(2)	0.271(3)	
O(1)	0.644(2)	0.499(1)	0.422(2)	
O(2)	0.751(3)	0.470(2)	0.197(2)	
O(3)	0.582(2)	0.306(2)	0.270(1)	
O(4)	0.514(2)	0.545(2)	0.198(2)	

Overall isotropic temperature factor 1.08(29)

$$\frac{\sum w\,(I_{obs} - I_{calc})^2}{\sum w\,I_{obs}^2} = 0.19\%$$

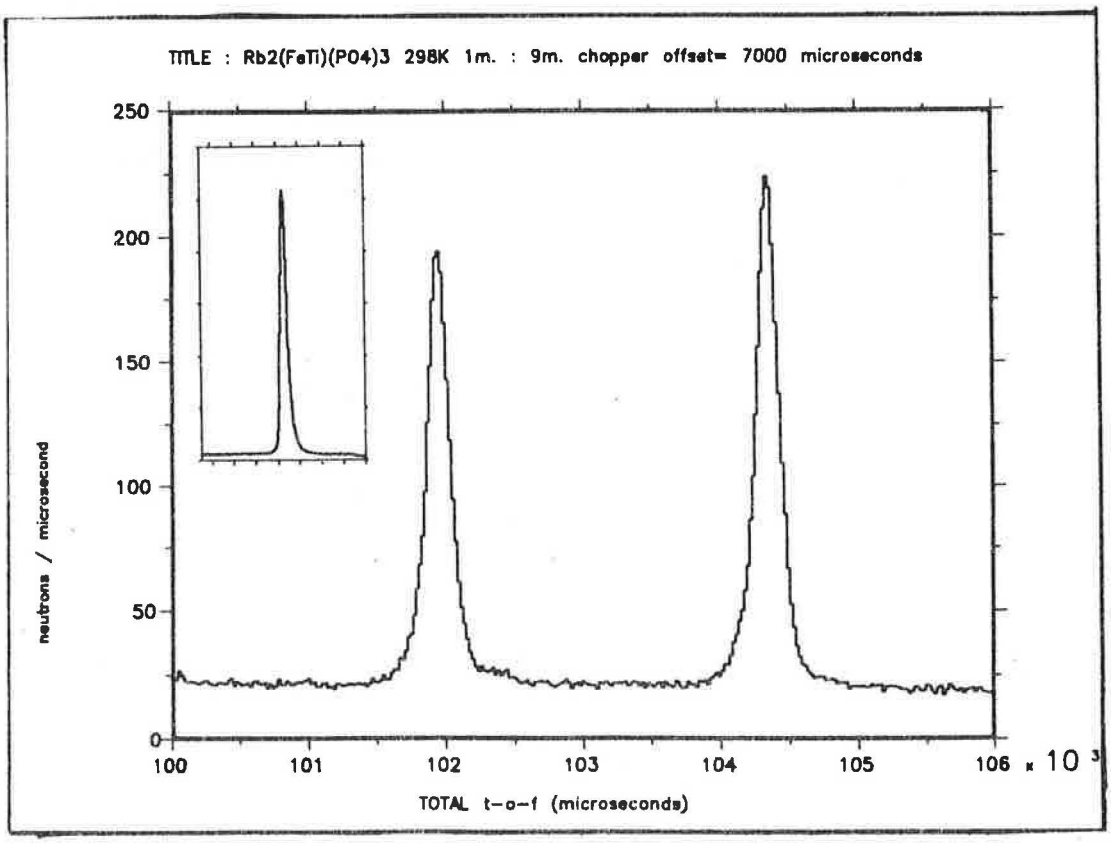

Figure 4: Typical Bragg peaks for langbeinite, $Pb_2FeTi(PO_4))_3$ showing the anisotropic beak broadening. Inset shows the peak shape recorded for a standard alumina sample under similar conditions.

AB INITIO STRUCTURE DETERMINATION

The single most important contribution to high resolution powder diffraction over the past decade is widely recognised to be the Rietveld method which has, with current machines, enabled complex structures with up to 100 parameters to be refined. Structure determination, however, has proved for the most part to be intractable as a routine procedure because of limited resolution and the resultant inability to resolve a sufficient number of independent intensities to allow analysis by direct methods or Patterson techniques. The new generation of instruments, such as HRPD, that possess ($\Delta d/d$) resolutions of better than 0.001, have, in principle, the resolving power to separate a sufficiently large set of reflections to permit structure determination. The successful determination of the structure of ferric arsenate, $FeAsO_4$, indicates that the most significant contribution of the new high-resolution machines may be the routine structure determination of moderately-complex materials that are unavailable or costly to produce as single crystals.

The determination of a structure, whether from single crystal or powder data, can best be understood in terms of five discrete steps:

1. Automatic indexing of the powder diffraction pattern.
   - determination of the crystal system and cell constants.

2. Identification of possible (perhaps several) space groups from systematic absences.

3. Evaluation of individual integrated intensities.
   - where N peaks overlap apportion intensities as I/N
   - assign a small intensity I_s for unobserved systematically present intensities where I_s is ~ 1/10th of the smallest observed intensity of similar d spacing.

4a. Extraction of structural information, from the Patterson function, consisting of orientation and/or positioning of fragments and polyhedra, followed by either 4b or 5.

4b. Solution of the phase problem and determination of an approximate structure by direct methods (e.g. MITHRIL [11]) for possible space groups.

5. Refinement, either from integrated intensities or by profile analysis of the approximate structure to obtain the final answer.

AB INITIO STRUCTURE DETERMINATION OF $FeAsO_4$

Preliminary analysis of the neutron powder diffraction pattern (Figure 5) of $FeAsO_4$ recorded on HRPD clearly indicated that $FeAsO_4$ possessed a complex crystal structure of low symmetry. Auto-indexing of the 20 highest d-spacing reflections using the Visser [12] program gave monoclinic cell dimensions:

$a = 7.5636$ A ; $b = 8.0795$ A ; $c = 5.0117$ A ; $\beta = 104.46°$

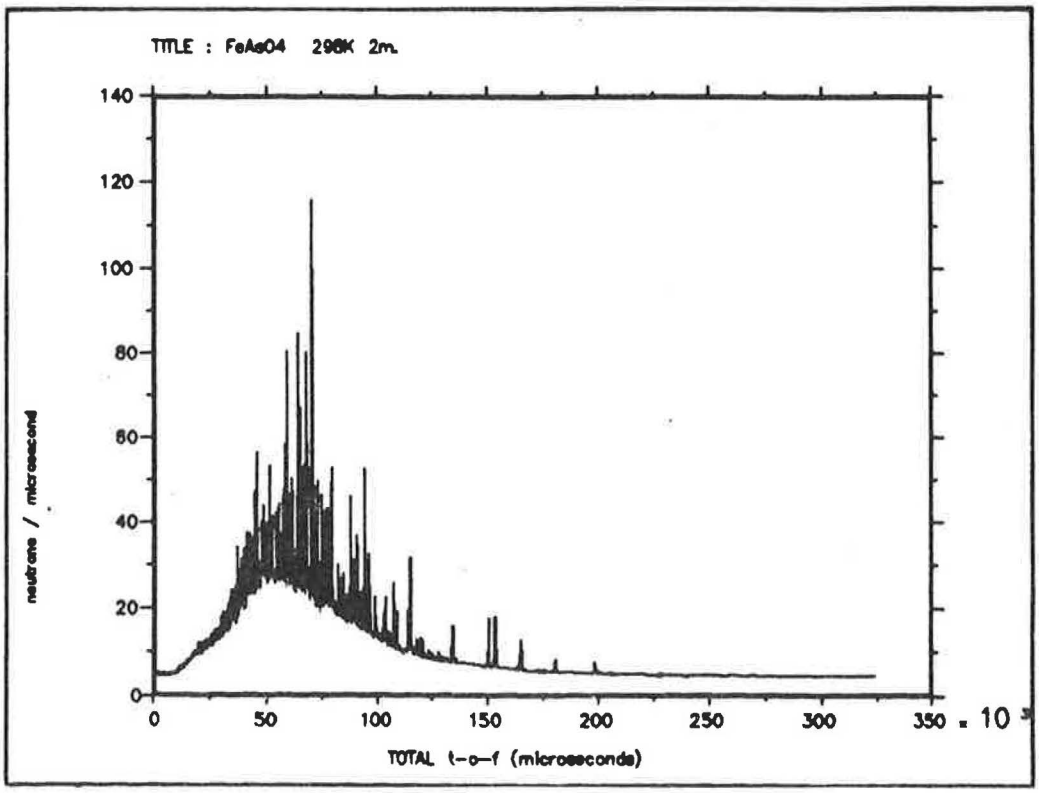

Figure 5: Raw time-of-flight diffraction data for ferric arsenate, $FeAsO_4$, showing the Bragg peaks superimposed on the spectral distribution of the incident beam.

With this information all 83 highest d-spacing peaks were indexed: systematic absences implied space group symmetry $P2_1/n$. The 83 peak areas were then used to provide input for the structure-solving direct methods program MITHRIL. The following tables show that six significant atomic sites were identified and readily allocated to iron (Fe), arsenic (As) and four oxygen (O) atoms according to peak heights.

Peak no.	Height	x/a	y/b	z/c
1	2691	0.177	0.449	0.758
2	1960	0.075	0.179	0.243
3	1320	0.131	0.256	0.913
4	1199	0.015	0.373	0.396
5	1193	0.898	0.046	0.178
6	1104	0.210	0.080	0.413
7	591	0.062	0.087	0.726
8	590	0.885	0.117	0.887

Atom	Scattering length (fm)	Expected height
Fe	9.54	2620
As	6.58	2130
O	5.81	1150

The above positional parameters were used as starting values for integrated peak intensities least-squares refinement. The optimised coordinates listed below correspond to the structure of $FeAsO_4$ illustrated below in Figure 6.

Atom	x	y	z
Fe	0.172(2)	0.460(2)	0.761(2)
As	0.071(3)	0.203(2)	0.219(4)
01	0.133(4)	0.268(3)	0.951(5)
02	0.026(4)	0.379(2)	0.385(5)
03	0.896(4)	0.076(3)	0.156(5)
04	0.240(3)	0.101(3)	0.414(4)

$$\frac{\sum w\,(I_{obs} - I_{calc})^2}{\sum w\,I_{obs}^2} = 0.7\%$$

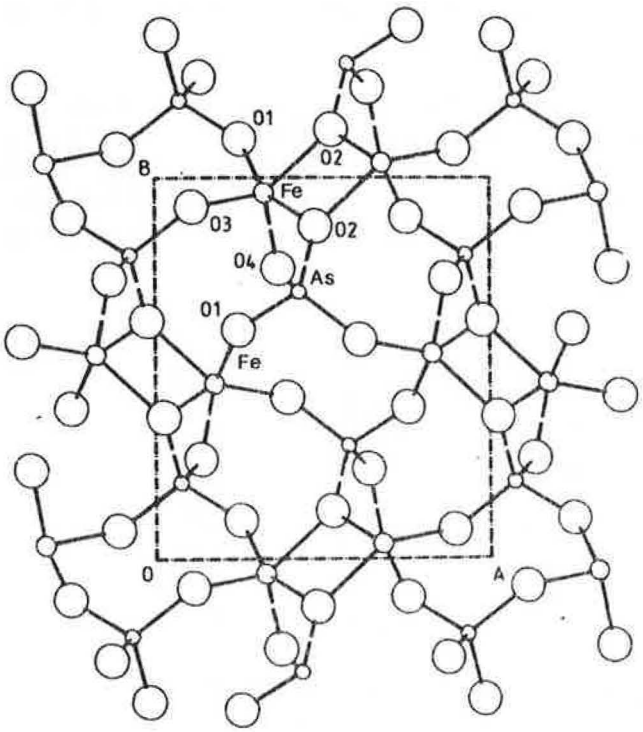

Figure 6: Projection of the crystal structure of $FeAsO_4$ viewed down [001], showing the edge-sharing FeO_5 units.

PROFILE ANALYSIS STRATEGY

We estimate that the enhanced resolution of HRPD will allow profile refinement of materials containing up to 400 structural parameters, as opposed to the limit of about 100 at present, although correct modelling of the peak shape and of wavelength dependent corrections is essential for reliable results. We have successfully refined the structures of standard titania and alumina (Figure 7) to weighted profile R-factors of ca 5%, using a simplified peak-shape algorithm assuming no Lorentzian sample contribution to the observed peak profile. Absorption and extinction corrections have at present been neglected. The Rietveld routines are being incorporated with standard crystallographic routines from the CCSL Library [8].

For a number of substances run on HRPD, the sample makes a major contribution to the peak shape and future algorithms must account for the anisotropic hkl dependence of this broadening which arises from the macroscopic properties of the sample. Indeed, the NBS 640a standard silicon sample [13] has shown hkl dependent broadening compared with the resolution observed for Al_2O_3 and NiO under identical experimental conditions. From its d-spacing dependence, this broadening may be attributed to strain rather than particle size effects. Even carefully prepared and relatively simple materials such as TeO_2 (Figure 8) show a complex hkl dependent peak broadening that has no obvious systematic behaviour. If the broadening is a result of particle size effects, then one possible strategy may be the microscopic examination of crystallites to determine their morphology. Having assigned crystal faces, say with the aid of diffraction, modelling of the average crystallite diffraction shape would be included in the profile refinement. A more pragmatic approach would be the refinement of integrated intensities from long d-spacing data in conjunction with profile refinement of the short d-spacing data where sample broadening is not so severe. We are examining the mathematical implications of such techniques at present.

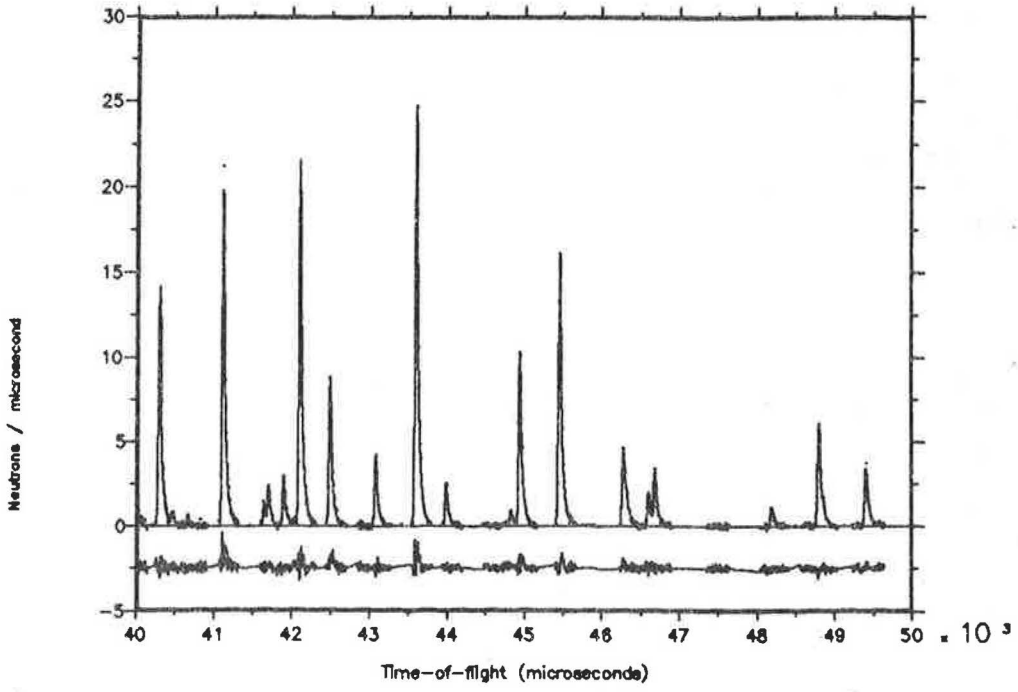

Figure 7: Final observed (points), calculated (line) and difference profile plots for alumina, Al_2O_3. This short section of the diffraction pattern corresponds to d-spacings between 0.8 and 1.0Å.

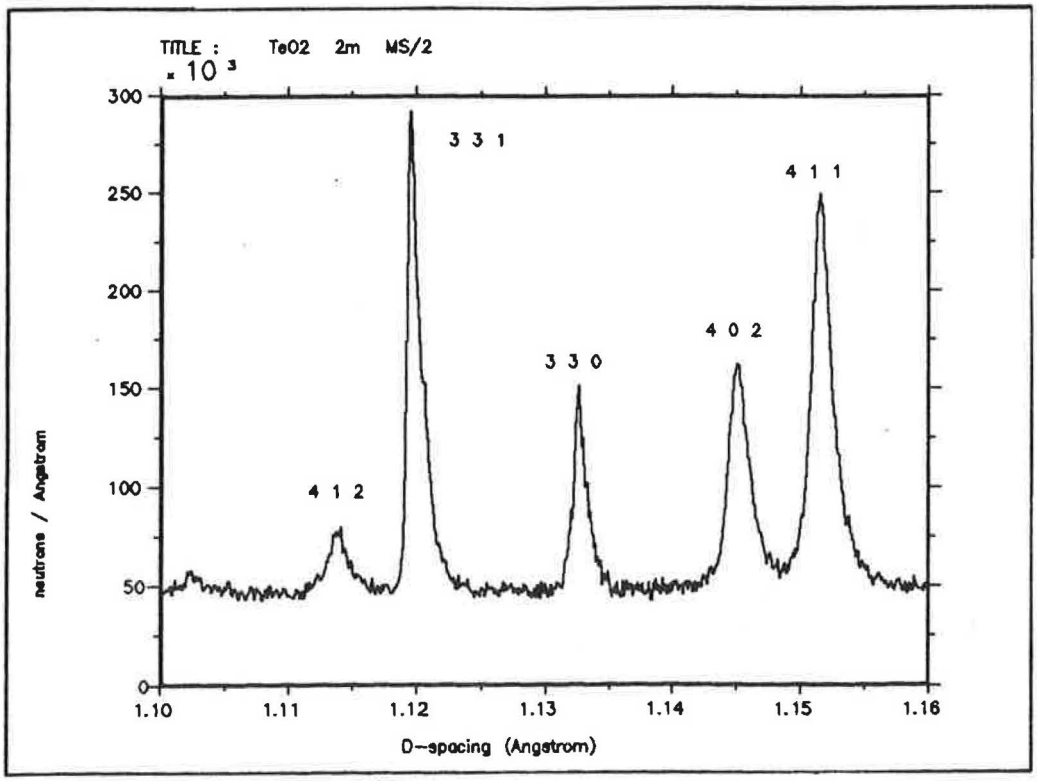

Figure 8: Section of the diffraction pattern of TeO_2 showing anisotropic peak broadening

CONCLUSIONS

The results presented in this paper are taken from experiments performed during commissioning and early user runs on HRPD between July 1985 and February 1986. During this time the ISIS proton current has increased from 0.1 μA to 10 μA (c.f. full design intensity of 200 μA). Extrapolation to full intensity indicates that run-times on HRPD will range from a few minutes to several hours for typical diffraction experiments. Preliminary data analysis has verified the theoretical resolution of less than 8×10^{-4} in $\Delta d/d$ over a range of d-spacings from 0.2 Å to 5 Å. High resolution 90° and 20° detectors are under consideration. These additional detector banks are optimised for special environment experiments, and will enable complete patterns to be collected in a single run out to d-spacings of ca 50 Å, whilst maintaining a resolution of 5×10^{-3} in $\Delta d/d$ from 5 Å upwards.

Initial experience on HRPD has clearly indicated that significant new science can be performed at resolutions of better than $\Delta d/d < 0.001$. The following topics represent perhaps the most exciting areas of future investigation:

a) large unit cell structures refinements with up to 300 refinable structure parameters
b) ab initio structure determination
c) phase transitions studies: subtle symmetry changes
d) line broadening investigations
e) high resolution special sample environment studies (e.g. high-pressure and partial-pressure experiments)
f) diffraction studies of incoherently scattering samples
g) anharmonic temperature measurements
h) automatic powder indexing and accurate lattice parameter determination.

ACKNOWLEDGEMENTS

We wish to thank the staff of Neutron and ISIS Divisions at the Rutherford Appleton Laboratory for their invaluable assistance over the last 6 years. ISIS is funded by the Science and Engineering Research Council.

REFERENCES

1) Jorgensen, J D and Rotella, F J: J Appl Cryst 1982, 15, 27.

2) Johnson, M W: To be published in Nucl Inst Meth 1986.

3) Taylor, A D: Rutherford Appleton Laboratory Report 84-120, 1984.

4) Ikeda, S and Carpenter, J M: Nucl Inst Meth 1985, A235, 553.

5) David, W I F: To be submitted.

6) Eddy, M M: Personal communication.

7) Steenstrup, S: Aust J Phys 1985, 38, 319.

8) Matthewman, J C, Thompson, P and Brown, P J: J Appl Cryst 1982, 15, 167.

9) Zeeman, A and Zeeman, J: Acta Cryst 1957, 10, 409.

10) Battle, P D, Cheetham, A K, Harrison, W T A and Long, G J: J Sol St Chem 1986, 62 16.

11) Gilmore, C G: J Appl Cryst 1984, 17, 42.

12) Visser, J W: J Appl Cryst 1969, 2, 89.

13) Hubbard, C R, Swanson, H E and Mauer, F A: J Appl Cryst 1975, 8, 45.